

# Vector-Quantized Graph Auto-Encoder

Yoann Boget<sup>1,3</sup>, Magda Gregorova<sup>2</sup>, and Alexandros Kalousis<sup>3</sup>

<sup>1</sup>*University of Geneva*

<sup>2</sup>*Center for Artificial Intelligence and Robotics (CAIRO), FHWS*

<sup>3</sup>*Geneva School for Business administration HES-SO*

June 14, 2023

## Abstract

In this work, we address the problem of modeling distributions of graphs. We introduce the Vector-Quantized Graph Auto-Encoder (VQ-GAE), a permutation-equivariant discrete auto-encoder designed to model the distribution of graphs. By exploiting the permutation-equivariance of graph neural networks (GNNs), our autoencoder circumvents the problem of the ordering of the graph representation. We leverage the capability of GNNs to capture local structures of graphs while employing vector-quantization to prevent the mapping of discrete objects to a continuous latent space. Furthermore, the use of autoregressive models enables us to capture the global structure of graphs via the latent representation. We evaluate our model on standard datasets used for graph generation and observe that it achieves excellent performance on some of the most salient evaluation metrics compared to the state-of-the-art.

## 1 Introduction

Graph generative models are a significant research area with broad potential applications. While most existing models focus on generating molecules for de novo drug design, there has been interest in using these models for tasks such as material design [31], protein design [13], code programming modeling [2], semantic graph modeling in natural language processing, [3, 21], and scene graph modeling in robotics [25]. Despite progress in graph representation and generative methods, modeling the underlying distribution of graphs remains challenging. The main challenges are due to the discrete nature of graphs, and the permutation-invariance property that learning methods need to achieve in order to efficiently learn from the different but equivalent representations of a graph.

To address these challenges, we propose a novel approach for graph generation based on a permutation-equivariant vector-quantized autoencoder. Our

approach encodes the graph into a set of node representations, each of which captures its local neighborhood. These representations are quantized to form a discrete latent space, from which the graph is decoded back to its original form. In this way, the autoencoder can be viewed as a function that encodes the graph into a set of discrete objects. Unlike graphs, which are particularly difficult to represent in a unique order, finite sets of objects can be easily sorted. Therefore, we can sort sets into unique latent representations and learn their distribution as sequences, capturing the global structure of the graph. Furthermore, to learn these sequences, we can leverage parallelizable autoregressive models such as transformers.

Our work makes three main contributions. Firstly, we identify the limitations of graph neural networks (GNNs) when used in autoencoders and propose solutions to overcome them. Secondly, building on these solutions, we introduce a permutation-equivariant autoencoder with a discrete latent space better suited for modeling discrete objects such as graph. Finally, we propose a new generative model, named Vector-Quantized Graph AutoEncoder (VQ-GAE), that achieves excellent performance in graph generation.

In the following section, we provide an overview of the background and problem statement of graph generative modeling. Specifically, we discuss the limitations of graph neural networks (GNNs) and several solutions proposed to overcome them. In the next section, we present the related works. We then introduce our Vector-Quantized Graph Auto-Encoder (VQ-GAE), which includes the details of the autoencoder architecture, the quantization process, and the autoregressive model used to learn the prior distribution. Finally, we present the experimental evaluation of our model and demonstrate its superior or competitive performance against the state-of-the-art on various types of graphs, including simple and annotated graphs.

## 2 Graph Representation Learning

In this section, we provide the necessary background for the method that we present. Firstly, we define the notation that we use and review the challenges of learning graph representations that mainly stem from the graph isomorphism problem. We then introduce graph neural networks and discuss some of their limitations.

### 2.1 Graphs notation and isomorphism

#### 2.1.1 Notation

We define a simple (unannotated and undirected) graph as a tuple  $\mathcal{G} = (\mathcal{V}, \mathcal{E})$ , where  $\mathcal{V}$  is the set of nodes, whose cardinality is  $n$ , and  $\mathcal{E}$  is the set of edges between these nodes. Given two nodes  $\nu_i$  and  $\nu_j$  in  $\mathcal{V}$ , we represent the edge connecting them as  $\epsilon_{i,j} = (\nu_i, \nu_j) \in \mathcal{E}$ . For annotated graphs, we introduce two additional functions  $V$  and  $E$  that map the nodes and the edges to their respective attributes:  $V(\nu_i) = \mathbf{x}_i$  and  $E(\nu_i) = \mathbf{e}_i$ . We denote an annotated

graph as  $\mathcal{G} = (\mathcal{V}, \mathcal{E}, V, E)$ . We use the notation  $\pi(\cdot)$  to specify that the graph, the set of nodes or the set of edges is represented under a particular node ordering.

### 2.1.2 Graph isomorphism

One of the main characteristics of graphs is their invariance to node permutations. In other words, any permutation in the ordering of the nodes yields the same graph. We can express this as:

$$\mathcal{G} = (\mathcal{V}, \mathcal{E}) \iff \pi(\mathcal{G}) = (\pi(\mathcal{V}), \pi(\mathcal{E})) \quad \forall \pi \in \Pi, \quad (1)$$

where  $\Pi$  is the set of all possible permutations over the set  $\mathcal{V}$ . Therefore, there are  $n!$  possible isomorphisms representing the same graph. Hence, the probability of a graph is the marginal distribution over all possible permutations:

$$p(\mathcal{G}) = \sum_{\pi \in \Pi} p(\pi(\mathcal{G})). \quad (2)$$

The permutation invariance graphs is at the core of the graph isomorphism in which we need to determine whether two graphs are the same or not. Solving the graph isomorphism problem is computationally expensive, and it is not known to be solvable in polynomial time [11]. Consequently, finding a unique way of representing a graph, which would solve the graph isomorphism problem, is also computationally expensive.

## 2.2 Graph neural networks

### 2.2.1 Graph Neural Networks

Graph Neural Networks (GNNs) provide an elegant solution to the node ordering problem. GNNs are neural networks that act as permutation-equivariant functions. A function  $f$  is permutation-equivariant if:

$$f(\pi(\mathcal{G})) = \pi(f(\mathcal{G})). \quad (3)$$

Notably, this implies that the input and output of the GNN have the same cardinality. Therefore, GNNs are said to be "flat". Furthermore, during training, the parameter update of GNN is permutation-invariant. A function is permutation-invariant if:

$$f(G) = x \implies f(\pi(\mathcal{G})) = x. \quad (4)$$

The invariance of the parameter update effectively eliminating the ordering problem.

Message Passing Neural Networks (MPNNs) [41], are a common type of GNN that operate in two steps. First, they compute messages from the neighborhood of each node, and then aggregate the messages to compute new node

representations. A layer of an MPNN computes new node representations as follows:

$$\mathbf{x}_i^{l+1} = \phi \left( \mathbf{x}_i^l, \bigoplus_{j \in \mathcal{N}(i)} \psi(\mathbf{x}_i^l, \mathbf{x}_j^l, \mathbf{e}_{ij}^l) \right), \quad \forall \mathbf{x}_i \in V(\nu_i) \quad (5)$$

where  $\phi$  and  $\psi$  are Multi-Layer Perceptrons (MLPs) and  $\bigoplus_{j \in \mathcal{N}(i)}$  denotes a permutation-invariant aggregation function over the neighborhood of node  $i$ .

In our study, we have introduced a modification to the standard message passing neural network (MPNN) architecture. As proposed in [8], we want to have access to intermediate edge representations and compute these independently from the message passing operation. Therefore, we first compute the new edge feature representations and then perform the classical message passing operation. We use a simple sum aggregation function. Thus, the layer output  $l+1$  of our GNNs is defined as follow:

$$\mathbf{e}_{i,j}^{l+1} = \text{bn}(f_{\text{edge}}(\mathbf{x}_i^l, \mathbf{x}_j^l, \mathbf{e}_{i,j}^l)) \quad (6)$$

$$\mathbf{x}_i^{l+1} = \text{bn} \left( \mathbf{x}_i^l + \sum_{j \in \mathcal{N}(i)} f_{\text{node}}(\mathbf{x}_i^l, \mathbf{x}_j^l, \mathbf{e}_{i,j}^l) \right), \quad (7)$$

where  $\text{bn}$  stands for *batch normalization* [14].

Despite their favorable properties regarding graph isomorphism problem, MPNNs present also some pitfalls. One significant issue is their susceptibility to oversmoothing, which occurs when the node and edge representations converge to the same value as the number of layers increases [24,35]. The depth of MPNNs needs to be limited, constraining the message passing. Additionally, standard MPNNs have limited representation power, making it difficult to differentiate between non-isomorphic graphs that share similar structural characteristics [34].

To enhance the representation power of our MPNN and overcome its limitations, we propose to aggregate information from the  $p$ -hop neighborhood, i.e. the neighborhood reachable with a path of at most  $p$  edges. To differentiate between the  $p$  levels of neighborhood, we augment the edge features with a  $p$ -dimensional vector, where the  $i^{\text{th}}$  entry corresponds to the number of  $i$ -paths connecting the two incident nodes. Similarly, we augment the node features with the  $i$ -degrees, which is the number of  $i$ -paths emanating from the node. To ensure computational efficiency, we set  $p$  to 3, which makes the path matrices easy and quick to compute. Furthermore, we need to perform this operation only during preprocessing. Our solution is closely related to the recent work presented in [6].

## 2.2.2 GNN-based graph auto-encoding

Autoencoders operate by learning to map their inputs to some latent representation and then decoding from the latent representation back to the original input. Due to their permutation-equivariance MPNNs are our model of choice

for a graph autoencoder; however using them in such a setting is not straightforward. MPNNs encode graphs by mapping them to a set of learned node representations. The learned encoding will introduce problems to the downstream decoder due to the presence of symmetries in the graphs that will make decoding challenging. In particular, when nodes have the same structural role within a graph their feature representations after passing through a MPNN will be identical; such nodes are known as regularly equivalent [38, 46]. Such cases arise when a graph contains a bipartite subgraph, formed by groups of regularly equivalent nodes connected by edges, and the bipartite graph is neither complete<sup>1</sup> nor without edges. As a result of the identical node representation it is not possible to reconstruct the original graph by only relying on the learned node representations. Figure 1 illustrates the problem. There we have two groups of regularly equivalent nodes. The representations of all potential edges between the two groups of nodes that have identical representation will be identical and the original graph cannot be reconstructed.

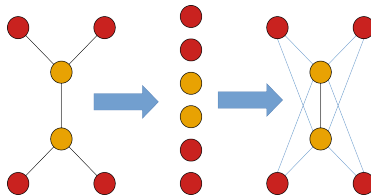


Figure 1: The original graph (depicted on the left) contains two groups of regularly equivalent nodes (nodes with the same color are regularly equivalent). When we encode such a graph as a multiset of nodes using a GNN, nodes of the same color will have the same representation. As a result, any function taking this multiset as argument and computing any kind of relation between its elements (as we do for decoding a graph) will return the same value for all the relations between the two groups (drawn in blue on the right). Consequently, the original graph cannot be accurately reconstructed.

To resolve the problem of regularly equivalent nodes when we encode graphs with MPNNs we concatenate a noise vector to the node attributes to break the symmetries in the graph when needed. Similar approaches have been previously proposed in [30, 40] in the case of supervised learning.

### 3 Related work

In this section we will briefly review existing work on graph generative models. We will make an explicit distinction between generative models for generic graphs and generative models for molecules. The latter class of works even though they do constitute a graph generation problem very often make explicit

<sup>1</sup>A bipartite graph is complete when every node of the first set is connected to every node of the second set

use of domain knowledge that is specific to molecules and chemistry. Such domain knowledge is not available in the general case. We will focus on generative models for generic graphs and discuss the two main approaches, auto-regressive generation and one-shot generation.

### 3.1 Molecule generative models

Molecule generation is an important application for graph generative modeling. Many graph generative models focus on molecule generation and often leverage extensive domain-knowledge. However, some works on molecule do not use a graph representation. The earliest works using deep learning operate over a sequential representation of the molecules such as the SMILES representation [10,22]. Some more recent models use 3D-based molecule representations [12]. In this work, we specifically focus on graph generative models and are interested in developing generic graph modeling techniques. Thus, we will only review models that use a graph representation for molecule generation, and omit other approaches such as sequential or 3D representations.

### 3.2 Autoregressive graph generation

A common approach consists of generating graphs in an autoregressive manner one-building-element at the time. Depending on the method the building elements can be nodes and edges but also more complex structures such as sub-graphs. As previously mentioned, one of the primary challenges with autoregressive models is establishing an appropriate ordering/canonical representation of the graph, i.e. establish a canonical sequence of the building blocks. At the same time they are slow both at training and inference (see results in [18]) and introduce long-range dependencies. GraphRNN [48] is one of the first works that took such an approach. Instead of finding a unique representation for each graph, which would require solving the graph isomorphism problem, the authors propose shrinking the number of possible ways of representing the graph by following the ordering of a breadth-first search algorithm (BFS). However, the model still needs to learn all possible ordering from the BFS. Other autoregressive models use a unique representation [9], generate the graphs block-by-block to accelerate the generation process [27] or use a canonical ordering that is domain dependent [26].

Autoregressive models have also been combined with latent variable models, particularly with variational autoencoders [16, 17, 29, 39] and flows [23, 32, 42]. All these models have been specifically developed for molecule generation and make use of domain knowledge, although [32, 42] are also capable of handling non-annotated graphs.

### 3.3 One-shot graph generation

By 'one-shot graph generation', we refer to models where the generative function outputs the entire graph at once, as opposed to computing it incrementally

from subgraphs, which would require an ordering. These models exploit the permutation-equivariance or permutation-invariance property of MPNNs and are thus insensitive to the ordering of the graph representations in the dataset.

This approach includes models based on Generative Adversarial Networks (GANs) [1, 5], Variational Autoencoders (VAEs) [7, 43], flows [28, 33, 49], or score-based models [18, 47].

MolGAN [5], the unique GAN-based model, uses MPNN for the discriminator only. The generator is a simple multi-layer perceptron, which does not prevent it from generating graphs in different orderings. We presume that this exacerbates the known difficulties of training GANs. Indeed, the authors report mode collapse and poor results in terms of the diversity of the generated graphs. One-shot flow-based models that use dequantization to transform graphs into continuous objects have been shown to produce better results [49].

Score-based models, on the other hand, introduce noise to the original graphs and assume a fully connected graph, allowing all nodes to directly share information with each other. This approach captures the global structure of the graph effectively and has produced the best results to date, with [18] being considered the current state-of-the-art. However, the numerous denoising steps required in score-based models make the generation process slow.

In contrast to both autoregressive and continuous latent variable models, one-shot VAE models for graph generation, such as those proposed in [43] and [7], do not use permutation-equivariant functions end-to-end. Instead, they use a unified latent space for the whole graph, resulting in the loss of node ordering information. As a result, a matching procedure is required to evaluate the reconstruction loss, making this approach computationally expensive. Unlike these models our autoencoder is end-to-end permutation-equivariant eluding the need for a matching procedure.

## 4 Vector-Quantized Graph Auto-Encoder

Our objective is to model the distribution of graphs, which are discrete objects (assuming their attributes are also discrete). When encoding discrete objects into a latent space, the resulting space is also discrete, even if it is represented in a continuous vector space. In contrast, decoding continuous latent variables back into discrete objects requires a discretization process. As a consequence, certain operations in the latent space, such as interpolation, have no meaningful interpretation in the space of discrete objects. Thus, we argue that discrete latent spaces are better suited for modeling discrete objects such as graphs.

Moreover, due to the limitations of GNNs, it may not be feasible to directly map the original distribution over graphs to a known variational distribution as in standard variational auto-encoders [20]. Instead, we propose encoding graphs into sets of node embeddings, implicitly defining an unknown latent distribution. Quantization of the elements in the sets restricts the size of the latent space, thereby aiding in learning the complex relationships between the elements of the latent variables. Figure 2 depicts a sketch of our autoencoder. Although

motivated by different considerations, our model appears to be closely related to the VQ-VAE [44]. In the following, we provide a detailed description of the various components of our model and highlight the particularities related to graph modeling. Figure 2 depicts a sketch of our model.

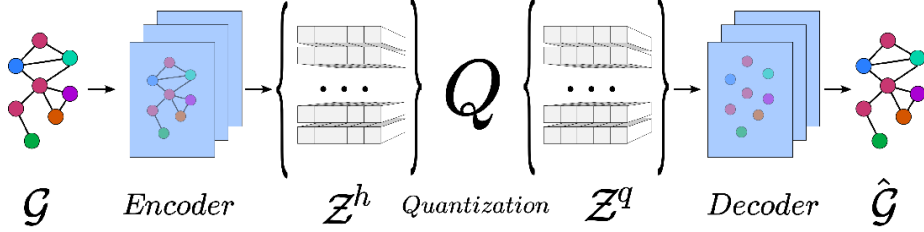


Figure 2: We encode a graph into a set of node embeddings, each consisting of  $c$  vectors that are quantized by mapping them to the nearest neighbor in a codebook. We then decode the resulting quantized set to recover the original graph. [Note: A better version of the sketch will be presented for the final version.]

#### 4.1 Auto-encoder

The auto-encoder consists of an encoder and a decoder. The encoder is a standard MPNN as described in a previous section. It encodes the input graph into a latent space, which consists of  $n$  latent vectors representing each node in the graph. Due to the permutation-equivariance property of the MPNN, the encoder can be seen as a graph-to-set function  $f(\mathcal{G}) = \mathcal{Z}^h$ . The set  $\mathcal{Z}^h$  contains the  $n$  node latent representations  $\mathcal{Z}^h = \{Z_1^h, \dots, Z_n^h\}$ . The  $\mathcal{Z}$  with the superscript  $h$  indicates the set before quantization. We will use the superscript  $q$  to refer to the quantized latent representations. The bottleneck of our auto-encoder, in addition to the quantization process described in section 4.2 is the loss of the original graph structure. Therefore, the latent representations must encode not only the node features, but also their surrounding graph structure, such as the connections to other nodes, for accurate reconstruction.

After quantization  $Q : \mathcal{Z}^h \mapsto \mathcal{Z}^q$ , the decoder has to recover the graph structure and, optionally, the node and edge attributes. Since we have lost the connectivity in the latent space, we assume a fully connected graph among the elements of  $\mathcal{Z}^q$ . We subsequently feed the fully connected graph into a MPNN similar to the one used as encoder.

For simple graphs, the edge representation  $e_{i,j}^L$  after the last layer  $L$  is passed through a sigmoid function, yielding the probability of the presence of an edge for each potential edge  $\text{sigmoid}(e_{i,j}^L) = p(\hat{e}_{i,j}|\mathcal{G})$ . In the case of annotated graphs with discrete attributes, the outputs corresponding to each edge  $\mathbf{e}_{i,j}^L$  and each node  $\mathbf{x}_i^L$  are passed through a softmax function, yielding the probability distribution over their attributes, i.e.,  $\text{softmax}(\mathbf{e}_{i,j}^L) = p(\hat{\mathbf{e}}_{i,j}|\mathcal{G})$  and  $\text{softmax}(\mathbf{x}_i^L) = p(\hat{\mathbf{x}}_i|\mathcal{G})$ .



Since the auto-encoder is permutation-equivariant end-to-end, the outputs order match the input order, making the computation of the loss straightforward. For sampling, we always choose the mode of the distribution. The details about the auto-encoder architecture are given in the appendix B.

## 4.2 Quantization

The task at hand is to design a quantization process for the node embeddings that is both flexible and efficient. To achieve this goal, we propose to partition the node embedding into  $c$  vectors  $Z_i^h = (\mathbf{z}_{i,1}^h, \dots, \mathbf{z}_{i,c}^h) \in \mathbb{R}^{c \times d}$ , where  $d$  is the latent dimension of the  $c$  vectors. We then quantize each vector independently. This approach allows for flexibility in capturing the information contained in the embeddings while keeping the codebook size  $K$  reasonably small to maintain efficient learnability of the prior. This results in each node embedding being able to take  $K^c$  distinct values. Notably, even with a small  $c$  value, the representation power of the node embedding is drastically increased. In all of our experiments, we set  $c$  to a maximum of 2. Figure 3

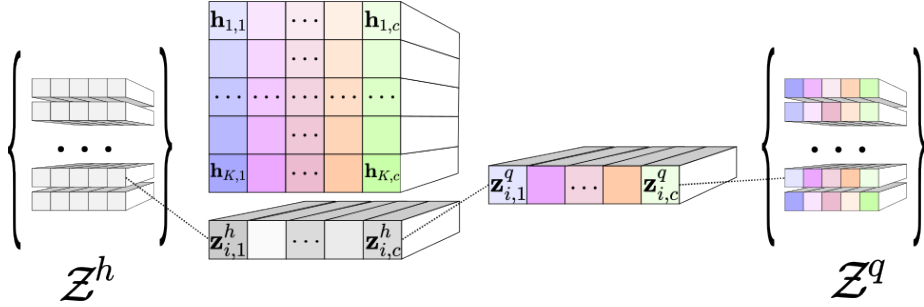


Figure 3: Each vector of the node embeddings is replaced by its closest neighbor from a the corresponding codebook. The vectors composing the codebooks are parameters, which are learned during training.

The latent representations  $Z^h$ , composed of  $n \times c$  vectors, are subsequently mapped to their nearest neighbors  $\mathbf{h}_{i,j}$  from a set of  $c$  codebooks ( $H_1$  to  $H_c$ , with  $H_i \in \mathbb{R}^{K \times d}$ ), distinct for each of the  $c$  vectors representing a node embedding. Specifically, we define the quantization function  $q(\mathbf{z}_{i,j}^h)$  as the mapping of the  $j$ -th vector of the embedding of node  $i$ ,  $\mathbf{z}_{i,j}^h$ , to its closest neighbor  $\mathbf{h}_{j,g}$  in the corresponding codebook  $H_j$ , according to:

$$q(\mathbf{z}_{i,j}^h) = \mathbf{z}_{i,j}^q = \mathbf{h}_{j,k} \quad \text{with} \quad k = \arg \min_g (\mathbf{z}_{i,j}^h - \mathbf{h}_{j,g}). \quad (8)$$

This approach differs from the conventional VQ-VAE model by using multiple codebooks, with each codebook specific to one of the  $c$  vectors representing a node embedding.

Notably, the quantization procedure is permutation-equivariant, as demonstrated in the appendix A. Additionally, this quantization process implicitly establishes a discrete distribution over sets of  $c$ -tuples.

### 4.3 Auto-encoder training

The autoencoder is trained using three proposed terms by [44], namely the reconstruction loss, the commitment loss, and the VQ loss. The reconstruction loss is defined as the negative log-likelihood of the generated graph given the quantized node embeddings, represented by  $\mathcal{Z}^q$ :

$$\mathcal{L}_{recon.} = -\mathbb{E} \left( \log p(\hat{\mathcal{G}} | \mathcal{Z}^q) \right) \quad (9)$$

Depending on the nature of the graph, we model the underlying distribution as a product of Bernoulli distributions over all possible edges for simple graphs or as a product of categorical distributions for graphs with discrete node and edge attributes. Appendix 2 provides additional details on the model formulation and implementation.

The commitment and VQ losses follow closely the formulation of the original VQ-VAE [44]:

$$\mathcal{L}_{VQ} = \frac{1}{nc} \sum_{i=1}^n \sum_{j=1}^c \|sg[\mathbf{z}_{i,j}^h] - \mathbf{h}_{k,j}\|_2^2 \quad (10)$$

$$\mathcal{L}_{commit.} = \frac{1}{nc} \sum_{i=1}^n \sum_{j=1}^c \|\mathbf{z}_{i,j}^h - sg[\mathbf{h}_{k,j}]\|_2^2, \quad (11)$$

where  $sg[\cdot]$  denotes the stop-gradient operation.

Putting the three components together, the total loss is given by the reconstruction loss plus a weighted sum of the commitment and VQ losses.

$$\mathcal{L}_{tot.} = \mathcal{L}_{recon.} + \gamma(\mathcal{L}_{VQ} + \beta\mathcal{L}_{commit.}) \quad (12)$$

We introduce the weighting parameter  $\gamma$  to balance the contribution of the commitment and VQ losses to the overall loss and set it to 0.1. We use the value proposed by [44] for  $\beta$ : 0.25.

### 4.4 Prior learning

The process of auto-encoding implicitly defines a distribution over the latent space, which can be interpreted as a prior. To sample instances from this unknown distribution, it is necessary to learn it. In our case, we seek to learn a distribution over multisets of discrete objects, specifically node embeddings denoted by  $\mathcal{Z} = Z_1, \dots, Z_n$ , where each  $Z_i = (\mathbf{z}_{i,1}, \dots, \mathbf{z}_{i,c})$  is a  $c$ -tuple of quantized embeddings.

There are currently few generative models for sets and those that exist only deal with sets of continuous objects [19]. To the best of our knowledge, there

is currently no model that can directly handle (multi)sets of discrete objects. Therefore, we adopt the approach of transforming sets into sequences, which has the added advantage of maintaining fidelity with the original formulation of the VQ-VAE by fitting an autoregressive model to learn the prior. A critical aspect of this approach is the sequentialization of the set  $\mathcal{Z}$ .

In the following, we first present the process of sequentializing  $\mathcal{Z}$  and then describe the autoregressive model itself.

#### 4.4.1 Sequentialization

Firstly, we consider allowing the model to learn any ordering of the set. However, this option requires the model to learn any permutation of the set, which is not feasible in practice. Indeed, since there are  $n!$  possible permutations of a set of  $n$  elements, the model rapidly loses its capacity. As a result, this option is not realistic in practice.

An easy way of fixing an ordering over the set  $\mathcal{Z}$  consist of sorting the tuples  $Z_i$  according to the indices of their vectors in the codebooks. This sorting operation is a specific kind of permutation, which we refer to as  $\pi_s$ . Since the decoder  $f_d$  is permutation-equivariant by construction, it follows that  $f_d(\pi_s(Z^q)) = \pi_s(f_d(Z^q))$ . Furthermore, according to Equation 1, the permutation  $\pi_s(\mathcal{G})$  of the generated graph, as any permutation, yields the same graph as the original one, albeit in a different representation. So, there is no need to permute the graph back to its original ordering.

In practice, we map each vector  $\mathbf{z}_{i,j}^q$  to its index in the corresponding codebook. Since there is a bijection between the  $c$ -tuples of vectors  $(\mathbf{z}_{1,i}^q, \dots, \mathbf{z}_{c,i}^q)$  and the  $c$ -tuples of their corresponding indices in the codebook, there exists a unique  $c$ -tuple of indices for each possible  $Z_i$ . To perform the sorting operation, we use the index of the first element of each tuple as the primary criterion, the index of the second element as the secondary criterion, and so on.

Additionally, given the presence of an ordered sequence, we can leverage masking techniques to restrict the model from generating vectors with indices lower than the preceding element in the sequence.

#### 4.4.2 Autoregressive model

We can now model the probability of

$$Z^q = (Z_1^q, \dots, Z_n^q) = (\mathbf{z}_{1,1}^q, \dots, \mathbf{z}_{c,1}^q), \dots, (\mathbf{z}_{1,n}^q, \dots, \mathbf{z}_{c,n}^q) \quad (13)$$

as a sequence with an autoregressive model

$$p((\mathbf{z}_{1,1}^q, \dots, \mathbf{z}_{c,1}^q), \dots, (\mathbf{z}_{1,n}^q, \dots, \mathbf{z}_{c,n}^q)) = \prod_{i=1}^n \prod_{j=1}^c p(\mathbf{z}_{i,j}^q | \mathbf{z}_{<i, \cdot}^q, \mathbf{z}_{i, <j}^q) \quad (14)$$

To model this distribution, we use a model based on the blocks of a transformer [45]. As stated in the paper, compared to other autoregressive methods for sequence, transformers blocks improve: the total computational complexity

per layer, the amount of computation that can be parallelized as measured by the minimum number of sequential operations required, and the path length between long-range dependencies.

Therefore, we implement our model following the description of blocks in the original paper [45]. *'Each layer has two sub-layers. The first is a multi-head self-attention mechanism, and the second is a simple, position-wise fully connected feed-forward network. We employ a residual connection around each of the two sub-layers, followed by layer normalization'*. Similar to the transformer decoder, the node embeddings are offset by one position and we use masking to prevent from attending to subsequent positions. We also concatenate the non-offset sequence with the allowed vectors, i.e. the vectors  $\mathbf{z}_{i,j}$  with  $j$  smaller than the predicted ones. We use some common practices for sequence modeling such as padding, using an additional end-of-the-sequence token and positional-encoding.

After the transformer blocks, we pass the output through a last small feed-forward network with output size  $K + 1$  (the codebook size and an end-of-sequence token) followed by a softmax. The first element of the node embeddings being sorted, we also apply a masking before the softmax to prevent the model to assign any probability mass to vectors with a smaller index than the previous one in the sequence.

## 5 Evaluation

In this sections, we present the results of our experiments evaluating our model. We test our VQ-GAE on generation of both simple graph and annotated graph. For both types, we first present the datasets, the evaluation metrics and finally the results.

### 5.1 Simple graphs

#### 5.1.1 Evaluation

We evaluated the performance of our model on two small datasets, namely ego-small and community-small with respectively 200 and 100 graphs. We adopt the experimental procedure outlined in recent research [18]. Specifically, we employ the maximum mean discrepancy (MMD) to compare the distributions of graph statistics between generated and test graphs. We follow [48] and measure the distributions of degree, clustering coefficient, and the number of occurrences of orbits with 4 nodes. Similar to [18], we utilize the Gaussian Earth Mover's Distance (EMD) kernel to compute the MMDs.

The MMDs are computed by comparing the test set to generated samples of the same size as the test set. Our reported results are the average of 15 runs: 3 runs from 5 models trained independently.

### 5.1.2 Results

The results of our experiments on ego-small and community-small datasets are presented in Table 1. In the case of ego-small, which is a relatively small and straightforward dataset, we observe that our model matches the scores obtained with random samples from the training set. The lower score of GDSS [18] obtained on the MMD based on the clustering coefficient indicates overfitting of the test set. This could be due to the unfortunate absence of a validation set in the standard procedure and the limited size of the test set. We hypothesize that our two-step training approach (auto-encoder and prior training), reduces the risk of overfitting because the evaluation metrics cannot be used during the auto-encoder training.

On the community-small dataset, our model outperforms all baseline models in all evaluation metrics. We attribute this success to the effectiveness of our proposed VQ-GAE model.

In the appendix C, we provide more information about the datasets, the baselines, and we display visualizations of the graphs generated by our model for both experiments.

		Ego-small				Community-small			
<b>Model</b>		<b>Deg.↓</b>	<b>Clust.↓</b>	<b>Orbit↓</b>	<b>Avg↓</b>	<b>Deg.↓</b>	<b>Clust.↓</b>	<b>Orbit↓</b>	<b>Avg↓</b>
	Training set	0.022	0.043	0.0062	0.024	0.015	0.026	0.0032	0.015
Auto-reg.	GraphRNN	0.090	0.220	0.003	0.104	0.080	0.120	0.040	0.080
	GraphDF	0.04	0.13	0.01	0.060	0.06	0.12	0.03	0.070
	EDP-GNN	0.052	0.093	0.007	0.051	0.053	0.144	0.026	0.074
One-shot	GDSS	0.021	0.024	0.007	0.017	0.045	0.086	0.007	0.046
Ours	VQ-GAE	0.021	0.041	0.007	0.023	0.032	0.062	0.0046	0.033

Table 1: Generation results on datasets of simple graphs

## 5.2 Annotated graphs

### 5.2.1 Evaluation

We evaluated the performance of our model on two widely-used datasets for molecule generation: QM9 [37] and Zinc250k [15].

Traditionally, the evaluation of molecule generation was done through three metrics: validity, uniqueness and novelty. We argue that these metrics are not suitable for evaluation of the generative graph models.

Given that recent works mostly employ post hoc valency corrections that bring the validity rate to 100%, the validity rate has become an uninformative metric. Uniqueness and novelty primarily indicate potential mode collapse and overfitting, respectively. Since most models achieve a high score, these metrics provide little information for evaluation. Therefore, we do not focus on these

metrics in our evaluation. Nonetheless, for completeness, we produce these metrics in the appendix.

Instead, we focus on more appropriate evaluation metrics such as the Fréchet ChemNet Distance (FCD) [36] and the Neighborhood subgraph pairwise distance kernel (NSPDK) MMD [4]. As highlighted in [18] *'FCD and NSPDK MMD are salient metrics that assess the ability to learn the distribution of the training molecules, measuring how close the generated molecules lie to the distribution. Specifically, FCD measures the ability in the view of molecules in chemical space, while NSPDK MMD measures the ability in the view of the graph structure.'*

In addition to FCD and NSPDK metrics, we also include the validity rate without correction as a supplementary evaluation metric. This metric calculates the fraction of valid molecules without any valency correction or edge resampling, and we employ the version that allows for formal charge as in [18].

### 5.2.2 Results

As presented in Table 2, our VQ-GAE model exhibits superior performance compared to all other models in terms of FCD and NSPDK metrics, frequently surpassing them by a substantial margin. Moreover, it is competitive with the baselines in terms of validity without correction. We surmise that our model performs better at capturing global graph features while remaining competitive at capturing the local node-edge interactions necessary to generate valid molecules.

		QM9			ZINC		
Model		NSPDK↓	FCD↓	Valid. %↑	NSPDK↓	FCD↓	Valid. %↑
auto-reg.	GraphAF	0.021	5.53	74.4	0.044	16.0	68.5
	GraphDF	0.064	10.92	93.88	0.177	33.5	90.6
One-shot	MoFlow	0.017	4.47	91.4	0.046	20.9	63.1
	EDP-GNN	0.005	2.68	47.5	0.049	16.7	83.0
	GDSS	0.003	2.90	95.7	0.019	14.7	97.0
Ours	VQ-GAE	0.0023	0.80	88.0	0.008	5.4	65.7

Table 2: Generation results on molecular datasets

As for simple graphs, we provide more information about the datasets, the baselines, and we display visualizations of the graphs generated by our model for both experiments in the appendix C.

## 6 Conclusion

Our work introduces VQ-GAE, a permutation-equivariant discrete autoencoder specifically designed to handle the discrete nature of graphs without being af-

ected by the ordering of their representations. We utilize GNNs to capture the local structures of graphs and learn their global structures through the latent representations. Our experiments demonstrate the superior performance of our model on various tasks.

## References

- [1] Yoann Boget, Magda Gregorova, and Alexandros Kalousis. Graph annotation generative adversarial networks. In Emtiyaz Khan and Mehmet Gonen, editors, *Proceedings of The 14th Asian Conference on Machine Learning*, volume 189 of *Proceedings of Machine Learning Research*, pages 16–16. PMLR, 12–14 Dec 2023.
- [2] Marc Brockschmidt, Miltiadis Allamanis, Alexander L. Gaunt, and Oleksandr Polozov. Generative code modeling with graphs. In *International Conference on Learning Representations*, 2019.
- [3] Bo Chen, Le Sun, and Xianpei Han. Sequence-to-Action: End-to-End Semantic Graph Generation for Semantic Parsing. *ACL 2018 - 56th Annual Meeting of the Association for Computational Linguistics, Proceedings of the Conference (Long Papers)*, 1:766–777, 2018.
- [4] Fabrizio Costa and Kurt De Grave. Fast neighborhood subgraph pairwise distance kernel. In Johannes Fürnkranz and Thorsten Joachims, editors, *Proceedings of the 27th International Conference on Machine Learning (ICML-10), June 21-24, 2010, Haifa, Israel*, pages 255–262. Omnipress, 2010.
- [5] Nicola De Cao and Thomas Kipf. MolGAN: An implicit generative model for small molecular graphs. *arXiv:1805.11973 [cs, stat]*, May 2018. arXiv: 1805.11973.
- [6] Jiarui Feng, Yixin Chen, Fuhai Li, Anindya Sarkar, and Muhan Zhang. How powerful are k-hop message passing graph neural networks. In Alice H. Oh, Alekh Agarwal, Danielle Belgrave, and Kyunghyun Cho, editors, *Advances in Neural Information Processing Systems*, 2022.
- [7] Daniel Flam-Shepherd, Tony C. Wu, and Alan Aspuru-Guzik. MPGVAE: improved generation of small organic molecules using message passing neural nets. *Machine Learning: Science and Technology*, 2(4):045010, July 2021. Publisher: IOP Publishing.
- [8] Liyu Gong and Qiang Cheng. Exploiting edge features for graph neural networks. In *Proceedings of the IEEE/CVF conference on computer vision and pattern recognition*, pages 9211–9219, 2019.
- [9] Nikhil Goyal, Harsh Vardhan Jain, and Sayan Ranu. Graphgen: A scalable approach to domain-agnostic labeled graph generation. In Yennun Huang,

- Irwin King, Tie-Yan Liu, and Maarten van Steen, editors, *WWW '20: The Web Conference 2020, Taipei, Taiwan, April 20-24, 2020*, pages 1253–1263. ACM / IW3C2, 2020.
- [10] Rafael Gómez-Bombarelli, Jennifer N. Wei, David Duvenaud, José Miguel Hernández-Lobato, Benjamín Sánchez-Lengeling, Dennis Sheberla, Jorge Aguilera-Iparraguirre, Timothy D. Hirzel, Ryan P. Adams, and Alán Aspuru-Guzik. Automatic Chemical Design Using a Data-Driven Continuous Representation of Molecules. *ACS Central Science*, 4(2):268–276, February 2018. Publisher: American Chemical Society.
  - [11] Harald Andrés Helfgott, Jitendra Bajpai, and Daniele Dona. Graph isomorphisms in quasi-polynomial time, 2017.
  - [12] Emiel Hoogeboom, Victor Garcia Satorras, Clement Vignac, and Max Welling. Equivariant diffusion for molecule generation in 3d. In Kamalika Chaudhuri, Stefanie Jegelka, Le Song, Csaba Szepesvari, Gang Niu, and Sivan Sabato, editors, *Proceedings of the 39th International Conference on Machine Learning*, volume 162 of *Proceedings of Machine Learning Research*, pages 8867–8887. PMLR, 2022.
  - [13] John Ingraham, Vikas Garg, Regina Barzilay, and Tommi Jaakkola. Generative models for graph-based protein design. In H. Wallach, H. Larochelle, A. Beygelzimer, F. d'Alché-Buc, E. Fox, and R. Garnett, editors, *Advances in Neural Information Processing Systems*, volume 32. Curran Associates, Inc., 2019.
  - [14] Sergey Ioffe and Christian Szegedy. Batch normalization: Accelerating deep network training by reducing internal covariate shift. In Francis Bach and David Blei, editors, *Proceedings of the 32nd International Conference on Machine Learning*, volume 37 of *Proceedings of Machine Learning Research*, pages 448–456, Lille, France, 07–09 Jul 2015. PMLR.
  - [15] John J. Irwin, Teague Sterling, Michael M. Mysinger, Erin S. Bolstad, and Ryan G. Coleman. Zinc: A free tool to discover chemistry for biology. *Journal of Chemical Information and Modeling*, 52(7):1757–1768, 2012. PMID: 22587354.
  - [16] Wengong Jin, Regina Barzilay, and Tommi Jaakkola. Junction tree variational autoencoder for molecular graph generation. In Jennifer Dy and Andreas Krause, editors, *Proceedings of the 35th International Conference on Machine Learning*, volume 80 of *Proceedings of Machine Learning Research*, pages 2323–2332. PMLR, 10–15 Jul 2018.
  - [17] Wengong Jin, Regina Barzilay, and Tommi Jaakkola. Hierarchical Generation of Molecular Graphs using Structural Motifs. In *37th International Conference on Machine Learning, ICML 2020*, volume PartF16814, pages 4789–4798, 2020.



- [18] Jaehyeong Jo, Seul Lee, and Sung Ju Hwang. Score-based Generative Modeling of Graphs via the System of Stochastic Differential Equations. *Proceedings of the 39th International Conference on Machine Learning*, 162:10362–10383, 2022.
- [19] Jinwoo Kim, Jaehoon Yoo, Juho Lee, and Seunghoon Hong. Setvae: Learning hierarchical composition for generative modeling of set-structured data. In *Proceedings of the IEEE/CVF Conference on Computer Vision and Pattern Recognition (CVPR)*, pages 15059–15068, June 2021.
- [20] Diederik P Kingma and Max Welling. Auto-encoding variational bayes, 2022.
- [21] Matthew Klawonn and Eric Heim. Generating Triples With Adversarial Networks for Scene Graph Construction. *Proceedings of the AAAI Conference on Artificial Intelligence*, 32(1):6992–6999, apr 2018.
- [22] Matt J. Kusner, Brooks Paige, and José Miguel Hernández-Lobato. Grammar Variational Autoencoder. In *Proceedings of the 34th International Conference on Machine Learning*, pages 1945–1954. PMLR, July 2017. ISSN: 2640-3498.
- [23] Maksim Kuznetsov and Daniil Polykovskiy. MolGrow: A Graph Normalizing Flow for Hierarchical Molecular Generation. *Proceedings of the AAAI Conference on Artificial Intelligence*, 35(9):8226–8234, feb 2021.
- [24] Qimai Li, Zhichao Han, and Xiao-Ming Wu. Deeper insights into graph convolutional networks for semi-supervised learning. In *Proceedings of the Thirty-Second AAAI Conference on Artificial Intelligence (AAAI-18)*, pages 3538 – 3545, Palo Alto, CA, 2018-02. Association for the Advancement of Artificial Intelligence. 32nd AAAI Conference on Artificial Intelligence / 30th Innovative Applications of Artificial Intelligence Conference / 8th AAAI Symposium on Educational Advances in Artificial Intelligence; Conference Location: New Orleans, LA; Conference Date: February 2-7, 2018.
- [25] Y. Li, W. Ouyang, B. Zhou, K. Wang, and X. Wang. Scene graph generation from objects, phrases and region captions. In *2017 IEEE International Conference on Computer Vision (ICCV)*, pages 1270–1279, Los Alamitos, CA, USA, oct 2017. IEEE Computer Society.
- [26] Yujia Li, Oriol Vinyals, Chris Dyer, Razvan Pascanu, and Peter Battaglia. Learning deep generative models of graphs. In *ICLR 2018, 6th International Conference on Learning Representations*, feb 2018.
- [27] Renjie Liao, Yujia Li, Yang Song, Shenlong Wang, Will Hamilton, David K Duvenaud, Raquel Urtasun, and Richard Zemel. Efficient Graph Generation with Graph Recurrent Attention Networks. In *Advances in Neural Information Processing Systems*, volume 32. Curran Associates, Inc., 2019.

- [28] Jenny Liu, Aviral Kumar, Jimmy Ba, Jamie Kiros, and Kevin Swersky. Graph normalizing flows. In *Advances in Neural Information Processing Systems*, volume 32, 2019.
- [29] Qi Liu, Miltiadis Allamanis, Marc Brockschmidt, and Alexander L Gaunt. Constrained Graph Variational Autoencoders for Molecule Design. *The Thirty-second Conference on Neural Information Processing Systems*, 2018.
- [30] Andreas Loukas. What graph neural networks cannot learn: depth vs width. In *International Conference on Learning Representations*, 2020.
- [31] Chengqiang Lu, Qi Liu, Qiming Sun, Chang Yu Hsieh, Shengyu Zhang, Liang Shi, and Chee Kong Lee. Deep Learning for Optoelectronic Properties of Organic Semiconductors. *Journal of Physical Chemistry C*, 124(13):7048–7060, apr 2020.
- [32] Youzhi Luo, Keqiang Yan, and Shuiwang Ji. GraphDF: A Discrete Flow Model for Molecular Graph Generation. *Proceedings of the 38th International Conference on Machine Learning*, 139:7192–7203, 2021.
- [33] Kaushalya Madhawa, Katushiko Ishiguro, Kosuke Nakago, and Motoki Abe. Graphnvp: An invertible flow model for generating molecular graphs, 2019.
- [34] Christopher Morris, Martin Ritzert, Matthias Fey, William L. Hamilton, Jan Eric Lenssen, Gaurav Rattan, and Martin Grohe. Weisfeiler and leman go neural: Higher-order graph neural networks. In *33rd AAAI Conference on Artificial Intelligence, AAAI 2019, 31st Innovative Applications of Artificial Intelligence Conference, IAAI 2019 and the 9th AAAI Symposium on Educational Advances in Artificial Intelligence, EAAI 2019*, volume 33, pages 4602–4609. AAAI Press, jul 2019.
- [35] Kenta Oono and Taiji Suzuki. Graph neural networks exponentially lose expressive power for node classification. In *International Conference on Learning Representations*, 2020.
- [36] Kristina Preuer, Philipp Renz, Thomas Unterthiner, Sepp Hochreiter, and Günter Klambauer. Fréchet chemnet distance: A metric for generative models for molecules in drug discovery. *Journal of Chemical Information and Modeling*, 58(9):1736–1741, 2018. PMID: 30118593.
- [37] Raghunathan Ramakrishnan, Pavlo O. Dral, Matthias Rupp, and O. Anatole von Lilienfeld. Quantum chemistry structures and properties of 134 kilo molecules. *Scientific Data*, 1(1):140022, August 2014. Number: 1 Publisher: Nature Publishing Group.
- [38] Ryan A. Rossi and Nesreen Ahmed. Role discovery in networks. *IEEE Transactions on Knowledge and Data Engineering*, 27:1112–1131, 2014.

- [39] Bidisha Samanta, Bidisha@iitkgp Ac In, Abir De, Vicenç Gomez, Pratim Kumar Chattaraj, Niloy Ganguly, Manuel Gomez-Rodriguez, Jana Gourhari, and Kumar Chattaraj. NEVAE: A Deep Generative Model for Molecular Graphs \*. *Journal of Machine Learning Research*, 21:1–33, 2020.
- [40] Ryoma Sato, Makoto Yamada, and Hisashi Kashima. Random features strengthen graph neural networks. *Proceedings*, pages 333–341, 1 2021.
- [41] Franco Scarselli, Gori Marco, Tsoi Ah Chung, Hagenbuchner Markus, and Monfardini Gabriele. The Graph Neural Network Model. *IEEE Transactions on Neural Networks*, 20, jan 2009.
- [42] Chence Shi\*, Minkai Xu\*, Zhaocheng Zhu, Weinan Zhang, Ming Zhang, and Jian Tang. Graphaf: a flow-based autoregressive model for molecular graph generation. In *International Conference on Learning Representations*, 2020.
- [43] Martin Simonovsky and Nikos Komodakis. GraphVAE: Towards Generation of Small Graphs Using Variational Autoencoders. *arXiv:1802.03480 [cs]*, February 2018. arXiv: 1802.03480.
- [44] Aaron van den Oord, Oriol Vinyals, and koray kavukcuoglu. Neural discrete representation learning. In I. Guyon, U. Von Luxburg, S. Bengio, H. Wallach, R. Fergus, S. Vishwanathan, and R. Garnett, editors, *Advances in Neural Information Processing Systems*, volume 30. Curran Associates, Inc., 2017.
- [45] Ashish Vaswani, Noam Shazeer, Niki Parmar, Jakob Uszkoreit, Llion Jones, Aidan N Gomez, Łukasz Kaiser, and Illia Polosukhin. Transformer: Attention is all you need. *Advances in Neural Information Processing Systems 30*, pages 5998–6008, 2017.
- [46] Douglas R. White and Karl P. Reitz. Graph and semigroup homomorphisms on networks of relations. *Social Networks*, 5(2):193–234, 1983.
- [47] Carl Yang, Peiye Zhuang, Wenhan Shi, Alan Luu, and Pan Li. Conditional Structure Generation through Graph Variational Generative Adversarial Nets. In *Advances in Neural Information Processing Systems*, volume 32, 2019.
- [48] Jiaxuan You, Rex Ying, Xiang Ren, William Hamilton, and Jure Leskovec. GraphRNN: Generating Realistic Graphs with Deep Auto-regressive Models. In *Proceedings of the 35th International Conference on Machine Learning*, pages 5708–5717. PMLR, July 2018. ISSN: 2640-3498.
- [49] Chengxi Zang and Fei Wang. MoFlow: An Invertible Flow Model for Generating Molecular Graphs. *Proceedings of the ACM SIGKDD International Conference on Knowledge Discovery and Data Mining*, 10:617–626, aug 2020.

## A Equivariance of quantization

We show that the quantization function  $Q(\mathcal{Z}) = q(\mathbf{z}_{i,j}^h) = \mathbf{z}_{i,j}^q \quad \forall \mathbf{z}_{i,j}^h \in \mathcal{Z}$ , where  $q$  is the function in equation 8, is permutation-equivariant. To prove it, it is sufficient to show that:

$$Q(\mathcal{Z}^h) = \mathcal{Z}^q \implies Q(\pi(\mathcal{Z}^h)) = \pi(\mathcal{Z}^q)$$

Let assume  $Q(\mathcal{Z}^h) = \mathcal{Z}^q$ , then we have:

$$\begin{aligned} Q(\pi(\mathcal{Z}^h)) &= Q(Z_{\pi(1)}^h, \dots, Z_{\pi(n)}^h) \\ &= ((q(\mathbf{z}_{\pi(1),1}^h), \dots, q(\mathbf{z}_{\pi(n),1}^h)), \dots, ((q(\mathbf{z}_{\pi(1),c}^h), \dots, q(\mathbf{z}_{\pi(n),c}^h))) \\ &= ((\mathbf{z}_{\pi(1),1}^q, \dots, \mathbf{z}_{\pi(n),1}^q), \dots, ((\mathbf{z}_{\pi(1),c}^q, \dots, \mathbf{z}_{\pi(n),c}^q)) \\ &= (Z_{\pi(1)}^q, \dots, Z_{\pi(n)}^q) \\ &= \pi(\mathcal{Z}^q) \end{aligned}$$

## B Model Implementation Details

In this section, we provide more details on the implementation of our model.

### B.1 Auto-Encoder

For the molecular datasets, the encoders are made of 3 GNNs layers (as described in equation 5 and 6) and the decoder of 4 GNNs layers. For the non-molecular dataset, we use encoders and decoders with 2 GNNs layers.

In all experiments, the intermediate representations  $\mathbf{e}_{i,j}^l$  and  $\mathbf{x}_i^l$  are vector of dimension 32.

The functions  $f_{edge}$  and  $f_{node}$  respectively in equation 5 and 6 are Multi Layer Perceptrons, with 3 hidden layers of size 128 for the molecular datasets and 64 for the others. We do not use batch normalization before the GNNs output. We use ReLU as activation function.

### B.2 Quantization

For all our experiments, the latent representation  $Z_i = (\mathbf{z}_{i,1}, \mathbf{z}_{i,2})$  is composed of 2 vectors with dimension 4. For the Zinc dataset, we used 2 codebooks of 32 vectors  $H_1, H_2 \in \mathbb{R}^{32 \times 4}$ . For the other datasets, we used 2 codebooks of 16 vectors  $H_1, H_2 \in \mathbb{R}^{16 \times 4}$ .

### B.3 Training

In all our experiments, we use a batch size of 32 and an Adam optimizer with betas parameter (0.9, 0.99). We use a starting learning rate of  $10^{-3}$ , except for

the training of the prior with the Zinc dataset, where we observed that we need a slightly smaller starting learning rate and set it to  $5 * 10^{-4}$ .

We used exponential learning rate decay, by dividing the learning rate by 2 every 25K iterations for the molecular datasets and every 10K iteration otherwise.

## C Experiments

### C.1 Datasets

The ego-small dataset is constructed by extracting ego-networks from the large citeseer networks, which are real-world social networks. The dataset comprises 200 graphs having between 4 and 18 nodes.

The community-small dataset is a purely synthetic dataset. The number of nodes in each graph is uniformly sampled from the set 12, 14, 16, 18, 20. Each graph is divided into two communities of equal size. The probability of edge intra-community is set to  $p_{intra} = 0.7$ , while the probability of edge between inter-communities is set to  $p_{inter} = 0.03$ , with the constraint of having at least one edge between communities. The standard version of this dataset contains 100 graphs.

The QM9 dataset [37] comprises 133,885 small organic molecules with up to nine heavy atoms, consisting of only four atom types, namely *C, O, N, F*. We followed the convention in previous works and employed the kekulized version of the dataset with three edge types (single, double, and triple). To reconstruct the molecules, we adopted the same procedure as in [18].

The Zinc250k dataset is a subset of the Zinc database [15] that includes 250,000 molecules with up to 38 heavy atoms of nine types. We also used the kekulized representation of this dataset.

#### C.1.1 Baselines

For simple graphs, we present the results of four baseline models in our experiments. The first model, GraphRNN [48], is an RNN-based auto-regressive model and is the paper that introduced the experiments and metrics we use. The second model, GraphDF [32], is a flow-based model that is currently the best auto-regressive model available. The third and fourth models are one-shot diffusion models, namely EDP-GNN [47] and GDSS [18]. EDP-GNN is originally designed for simple graphs, while GDSS can generate both simple and annotated graphs.

In addition to these models, we also randomly sample the same number of graphs from the training set as there are in the test set to use as baseline. We report the average MMDs between the test set and 15 random samples drawn from the training set.

For molecular graphs, we also present the results of four baseline models. We utilize GraphDF [32], which is the best autoregressive model available. Additionally, we evaluate MoFlow [49], a one-shot flow-based model, the version

of EDP-GNN [47] adapted by [18] to handle annotated graphs, and GDSS, another score-based model, which represented state-of-the-art so far. We take the results from [18].

## C.2 Detailed results

### C.2.1 QM9

Results are the means and the standard deviation of 3 runs. All results except VQ-GAE are taken from [18].

Model	NSPDK↓	FCD↓	Val. wo. corr. %↑
GraphAF	0.021 ± 0.003	5.53 ± 0.40	74.4 ± 2.6
GraphDF	0.064 ± 0.000	10.92 ± 0.0	93.8 ± 4.8
MoFlow	0.017 ± 0.003	4.47 ± 0.60	91.4 ± 1.2
EDP-GNN	0.005 ± 0.001	2.68 ± 0.22	47.5 ± 3.6
GDSS	0.003 ± 0.000	2.90 ± 0.28	95.7 ± 0.8
VQ-GAE	0.0022 ± 0.0000	0.75 ± 0.03	88.6 ± 0.97

Table 3: Generation results on the **qm9** dataset

Model	Uniqueness↓	Novelety.↓	Validity %↑
GraphAF	88.64 ± 2.37	86.59 ± 1.95	100.00 ± 0.00
GraphDF	98.58 ± 0.25	98.54 ± 0.48	100.00 ± 0.00
MoFlow	98.65 ± 0.25	94.72 ± 0.77	100.00 ± 0.00
EDP-GNN	99.25 ± 0.05	86.58 ± 1.85	100.00 ± 0.00
GDSS	98.46 ± 0.61	86.27 ± 2.29	100.00 ± 0.00
VQ-GAE	97.23 ± 0.18	78.27 ± 0.11	100.00 ± 0.00

Table 4: Generation results on the **qm9** dataset

### C.2.2 Zinc

Results are the means and the standard deviation of 3 runs. All results except VQ-GAE are taken from [18].

## C.3 Visualization

Model	NSPDK↓	FCD↓	Val. wo. corr. %↑
GraphAF	$0.044 \pm 0.005$	$16.0 \pm 0.5$	$68.5 \pm 1.0$
GraphDF	$0.177 \pm 0.001$	$33.5 \pm 0.2$	$90.6 \pm 4.3$
MoFlow	$0.046 \pm 0.002$	$20.9 \pm 0.2$	$63.1 \pm 5.2$
EDP-GNN	$0.049 \pm 0.006$	$16.7 \pm 1.3$	$83.0 \pm 2.7$
GDSS	$0.019 \pm 0.001$	$14.7 \pm 0.7$	$97.0 \pm 0.8$
VQ-GAE	$0.008 \pm 0.000$	$5.3 \pm 0.1$	$65.1 \pm 0.6$
0,007994 5,32607			

Table 5: Generation results on the **ZINC** dataset

Model	Uniqueness↓	Novelty↓	Validity %↑
GraphAF	$98.64 \pm 0.69$	$99.99 \pm 0.01$	$100.00 \pm 0.00$
GraphDF	$99.63 \pm 0.01$	$100.00 \pm 0.00$	$100.00 \pm 0.00$
MoFlow	$99.99 \pm 0.01$	$100.00 \pm 0.00$	$100.00 \pm 0.00$
EDP-GNN	$99.79 \pm 0.08$	$100.00 \pm 0.00$	$100.00 \pm 0.00$
GDSS	$99.64 \pm 0.13$	$100.00 \pm 0.00$	$100.00 \pm 0.00$
VQ-GAE	$99.96 \pm 0.01$	$99.97 \pm 0.00$	$100.00 \pm 0.00$

Table 6: Generation results on the **ZINC** dataset

Model	Degrees↓	Cluster.↓	Orbits↓	Average↓
Training set	0.022	0.043	0.0062	0.024
Auto-reg. GraphRNN	0.090	0.220	0.003	0.104
GraphDF	0.04	0.13	0.01	0.060
EDP-GNN	0.052	0.093	0.007	0.051
One-shot GDSS	0.021	0.024	0.007	0.017
Ours VQ-GAE	0.021	0.041	0.007	0.023

Table 7: Generation results on the **Ego-small** datasets

Model	Degrees↓	Cluster.↓	Orbits↓	Average↓
Training set	0.015	0.026	0.0032	0.015
autoregressive GraphRNN	0.080	0.120	0.040	0.080
GraphDF	0.06	0.12	0.03	0.070
EDP-GNN	0.053	0.144	0.026	0.074
One-shot GDSS	0.045	0.086	0.007	0.046
Ours VQ-GAE	0.032	0.062	0.0046	0.033

Table 8: Generation results on the **Community-small** dataset

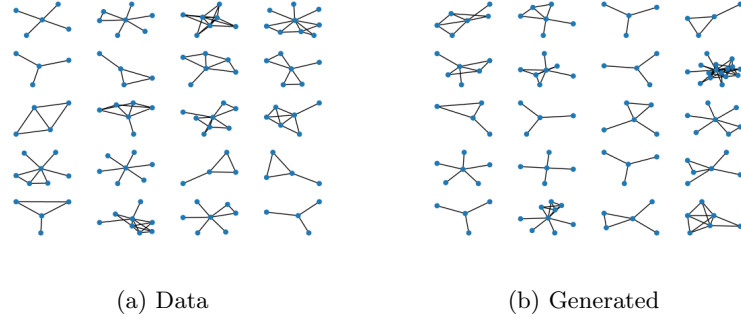


Figure 4: Example of graphs from the Ego-small dataset and from generated samples.

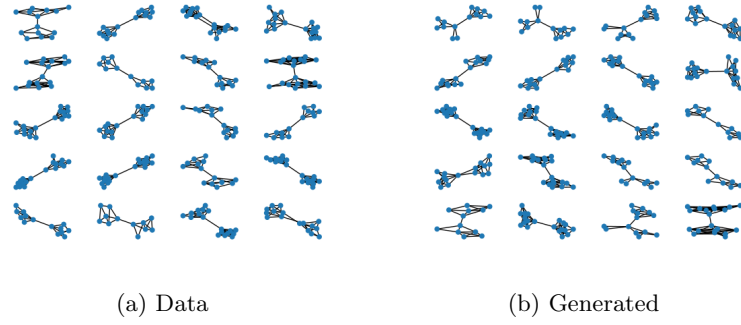


Figure 5: Example of graphs from the Community-small dataset and from generated samples.



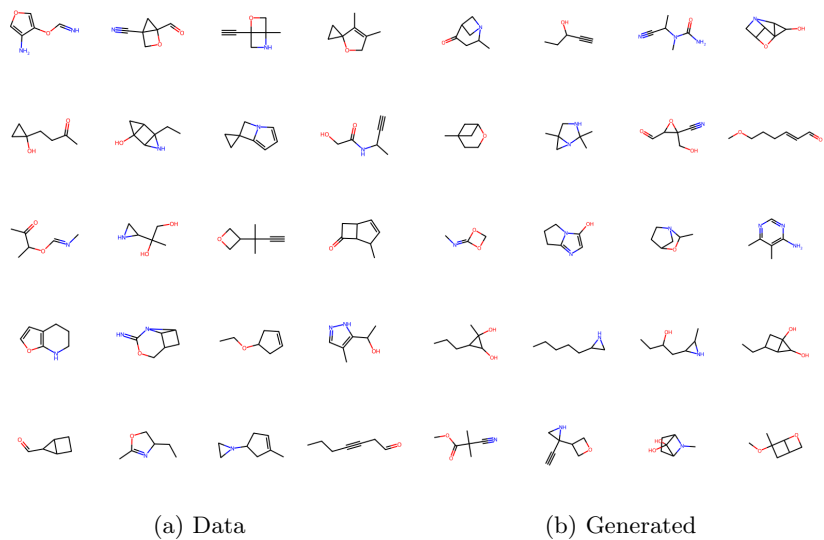


Figure 6: Example of graphs from the QM9 dataset and from generated samples.

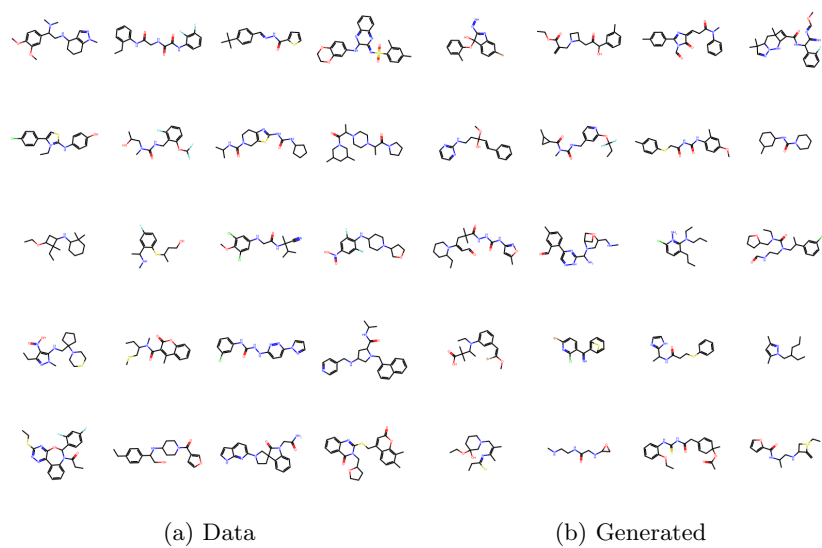


Figure 7: Example of graphs from the Zinc250K dataset and from generated samples.